

参赛队员姓名：张浚祈

中学：华南师范大学附属中学

省份：广东

国家：中国

指导教师姓名：杨晓安，欧阳柳章

指导教师单位：广东华南师范大学附属中学，华南理工大学材料科学与工程学院

论文题目：**Hydrogen generation from hydrolysis of borohydrides and its application in proton exchange membrane fuel cells**

2021 S.-T. Yau High School Science Award

# Hydrogen generation from hydrolysis of borohydrides and its application in proton exchange membrane fuel cells

Junqi Zhang<sup>a</sup>, Liuzhang Ouyang<sup>b,c,\*</sup>

<sup>a</sup>The Affiliated High School of South China Normal University

<sup>b</sup>School of Materials Science and Engineering, Guangdong Provincial Key Laboratory of Advanced Energy Storage Materials, South China University of Technology, Guangzhou, 510641, People's Republic of China. E-mail: [meouyang@scut.edu.cn](mailto:meouyang@scut.edu.cn).

<sup>c</sup>China-Australia Joint Laboratory for Energy & Environmental Materials, Key Laboratory of Fuel Cell Technology of Guangdong Province, Guangzhou, 510641, People's Republic of China.

## Abstract:

Hydrogen generation from the hydrolysis of  $\text{NaBH}_4$  or  $\text{LiBH}_4$  is among the most promising technologies for the realization of hydrogen economy. In the present study, we have developed a proton exchange membrane fuel cell (PEMFC) system integrated with  $\text{NaBH}_4/\text{LiBH}_4$  hydrogen source for portable electronic devices. By tailoring the concentration of  $\text{CoCl}_2$  solution from 0.05 to 0.5 wt%, a precise and controllable hydrogen generation rate up to  $4.2 \text{ L min}^{-1}$  is achieved, satisfying the requirements of different power PEMFCs. More specifically, a steady hydrogen flow ( $>0.4 \text{ L min}^{-1}$ ) can be attained to power a 30 W fuel cell that enables a 15 W LED display screen to light up by reacting  $\text{NaBH}_4$  with 0.1 wt%  $\text{CoCl}_2$  solution. With an

optimized dose of  $\text{CoCl}_2$  solution, a desirable gravimetric hydrogen density (GHD in short) of 7.0 wt%  $\text{H}_2$  with ~100% fuel conversion was realized at an  $\text{H}_2\text{O}:\text{SB} = 4:1$ , which may significantly improve the endurance ability of portable mobile powers with the same mass of fuel load. Moreover, it is cost-effective and convenient to regenerate  $\text{MBH}_4$  ( $\text{M} = \text{Li}, \text{Na}$  etc.) by ball milling the hydrolysis products ( $\text{MBO}_2 \cdot x\text{H}_2\text{O}$ ) with Mg-based reducing agents using green energy. By combining hydrogen generation, utilization and storage in a closed materials loop with a couple of  $\text{NaBH}_4/\text{LiBH}_4$  hydrolysis and regeneration, this study may offer new insight into deploying chemical hydrogen storage materials in portable mobile powers, especially for UAV.

**Keywords:** Borohydrides; Hydrogen generation; Hydrolysis; PEMFC; LED

2021 S.-T. Yau High School Science Award

## **Content:**

1. Introduction
2. Experimental sections
  - 2.1 Samples preparation and Apparatus
  - 2.2 Characterization
  - 2.3 Hydrolysis experiment
3. Result and Discussion
  - 3.1 Effect of  $\text{CoCl}_2$  concentrations on hydrogen generation kinetics of  $\text{NaBH}_4/\text{LiBH}_4$
  - 3.2 The gravimetric hydrogen density of  $\text{NaBH}_4$ -based system with a stoichiometric amount of  $\text{CoCl}_2$  solution
  - 3.3 The hydrogen generator integrated with a PEM fuel-cell stack and the application in LED
  - 3.4 Characterization of spent fuels and regeneration
4. Conclusion

### **1. Introduction**

The ever-increasing consumption of fossil fuels and the environmental issues caused by their combustion have led to the need to develop a new fuel system with outstanding renewability and sustainability, including nuclear energy <sup>1</sup>, solar energy <sup>2-3</sup>, hydrogen energy <sup>4-5</sup>, etc. Compared to many alternatives, hydrogen is regarded as the cleanest and

most reliable green energy alternative to fossil fuels because of its environmentally harmless product of oxidation which is  $\text{H}_2\text{O}$ , relatively ample energy density ( $142 \text{ MJ kg}^{-1}$ ), and renewability<sup>6-7</sup>. The advent of proton exchange membrane fuel cells (PEMFCs) creates the possibility of implementing hydrogen-based economy, enabling hydrogen applications from mobile electronic devices to medium-sized stationary power generators<sup>8-10</sup>. For the transformation of the world from the current hydrocarbon economy toward the so-called “hydrogen economy society”<sup>11-12</sup>, a major obstacle is that there are no efficacious hydrogen supply and storage methods in harnessing massive hydrogen. In this regard, developing safe, cost-effective, highly efficient hydrogen storage and evolution technologies is the linchpin for the commercial application of PEMFCs. Because of its poor energy density by volume, pure hydrogen is handled mainly in its pressurized state or liquid form. However, such processes greatly reduce the energy efficiency and pose a safety risk. Compared to ultrahigh-pressure or cryogenic-liquid hydrogen storage, materials-based solid hydrogen storage has received substantial attention because of higher hydrogen capacity, better safety, and milder operation conditions<sup>13-14</sup>.

Currently, both sodium borohydride ( $\text{NaBH}_4$ , SB)<sup>15-16</sup> and lithium borohydride ( $\text{LiBH}_4$ , LB)<sup>17-18</sup>, are the representative family members of complex metal hydrides and have been proposed as promising hydrogen storage media with the ideal hydrogen capacity of 10.8 wt% and 18.5 wt%, respectively. Unfortunately, it is highly challenging to achieve desirable reversible hydrogen capacity with mild conditions<sup>11, 19</sup>. Hydrogen supply from hydrolysis is an alternative strategy using single-use hydrogen carriers,

which is particularly attractive with a series of advantages that merit the practical hydrogen applications, such as mild operation temperature, precisely controlled hydrogen release, high-purity hydrogen, environmentally benign byproducts<sup>20</sup>. More specifically, hydrolysis of SB or LB is an on-site hydrogen supply method integrating hydrogen storage and production. The spent fuel can be readily regenerated back to the hydrogen carrier ex-situ. For example, SB forms a very stable aqueous solution with up to 30 wt% of SB (solubility limit) at room temperature, making it possible for long-term storage, safe transportation and real-time utilization. Moreover, H<sub>2</sub> can be released in a precisely controllable way using Co, Ni, Pt and other catalysts without any extra heat input<sup>21</sup>, and the slightly damp hydrogen can be transferred directly into PEMFCs without implementing any dehumidification process<sup>22</sup>. However, the actual hydrolysis of SB heavily depends on the dose of water, which is normally conducted in the aqueous phase. Therefore, typically, excess amount of water are needed<sup>16,23</sup>:



In this regard, the gravimetric hydrogen density (GHD in short) of SB is far lower than the theoretical value (10.8 wt%). This route is very attractive though the GHD is decreased to 4.0 wt% while using concentrated SB solution (>20 wt%), which is of practical interest for portable PEMFC applications, especially in small and medium (<2 kW) fuel cells. Both hydrolysis of SB or LB and fuel cells can operate under extremely quiet conditions, making it incredibly suitable for outdoor portable power generators, UAV, underwater vehicles, robots, or other military special applications.

Based on previous reports<sup>24-27</sup>, Co-based catalysts were considered as suitable

promoters for the hydrogen generation reaction due to their low cost and high catalytic activity. In the present work, we adopted LB and SB as hydrogen sources, and  $\text{CoCl}_2$  was used to accelerate the hydrogen kinetics. By tailoring the concentration of  $\text{CoCl}_2$  solution, a well-controlled hydrogen generation rate up to  $4.2 \text{ L min}^{-1}$  was achieved, which may meet the requirements of different power PEMFCs. Notably, a steady hydrogen flow can be achieved to power a 30 W fuel cell that enables a light-emitting diode (LED) to light up. Moreover, the GHD of SB and LB was explored with a stoichiometric amount of  $\text{CoCl}_2$  solution, aiming to improve the endurance ability of the fuel system. With the help of the fundamental research on LED display screen powered by SB-based hydrogen source integrated with 30 W fuel cell, it is able to further optimize SB-based fuel cell integrated system that enables UAV to drive stably with ideal flight endurance.

## **2. Experimental Sections**

### **2.1 Samples preparation and Apparatus**

Cobalt chloride hexahydrate ( $\text{CoCl}_2 \cdot 6\text{H}_2\text{O}$ , AR-grade) was purchased from Aladdin Chemical Company and were utilized to produce different concentrations of  $\text{CoCl}_2$  solution (0.05-0.5 wt%). SB (98 purity) and LB (95% purity) bought from Aladdin were utilized for hydrolysis. Active materials were processed in a glove box (Mikrouna, China) which generates an argon atmosphere with  $<1 \text{ ppm O}_2$  and  $\text{H}_2\text{O}$  vapor. Furthermore, the hydrolysates were exsiccated in an electrothermal blowing drying oven at  $60 \text{ }^\circ\text{C}$  for 12 h. A PEM stack (Zhangjiakou Hydrogen Technology Co., LTD,

30 W) was selected and used to power a LED (Henan Ricai Photoelectricity Shop, 15 W).

## 2.2 Characterization

Fourier transform infrared spectrometer (FTIR, Nicolet IS50) with a range of 400-4000  $\text{cm}^{-1}$  in the transmission mode was used to detect the chemical bonding of samples. The mixtures of sample and anhydrous potassium bromide (KBr) were cold-pressed with a 1:99 wt ratio, forming a disk. The spectra were generated from 16 averaged scans that possess a resolution of 4  $\text{cm}^{-1}$ . X-ray diffraction (XRD, PANalytical EMPYREAN) at 30 °C conducted by a Rigaku MiniFlex 600 with diffraction angles ( $2\theta$ ) which range from 10° to 90° with Cu-K $\alpha$  radiation (45 kV, 40 mA) at a scanning rate of 0.02°  $\text{s}^{-1}$  produces the graph of the phase structure of byproducts was gained via powder.

## 2.3 Hydrolysis Experiment

In the hydrolysis experiment, 0.05-0.1 g of reactants were put in a 50 mL sealed three-necked Pyrex flask with an outlet tube utilized to acquire the  $\text{H}_2$  gas. Then, the flask was immersed in a low-temperature reaction bath (Zhengzhou Great Wall Science and Technology Co., Ltd.) equipped with an circulating ethanol system to sustain the reaction temperature. Then the different concentrations of  $\text{CoCl}_2$  solution were injected to react with SB or LB to release hydrogen at a specific temperature. The water extracted is collected in a beaker placed on an electronic scale. The accuracy of it is 0.01 g, and the change of weight overtime is displayed by it as well. The hydrogen

generated is discharged via a Tygon tube and goes through the Monteggia washing bottle. Therefore, with the reaction time and hydrogen volume provided, the computer is able to analyze the data and calculate the rates and yields of hydrogen generation simultaneously. For practical applications, 1-5 g SB or LB was used to react with 20 mL of 0.1 wt%  $\text{CoCl}_2$  solution. Then the hydrogen generated can be used to power a 30 W fuel cell to light up the LED display screen.

### 3 Results and discussion

#### 3.1 Effect of $\text{CoCl}_2$ concentrations on hydrogen generation kinetics of $\text{NaBH}_4/\text{LiBH}_4$

To meet the requirements of diversified applications which need electricity, it is necessary to design stable and controllable hydrogen generation systems matching PEMFCs of different power. Concerning the sufficient heat capacity of a large amount of water, here, an excess amount of  $\text{CoCl}_2$  solution with a wide range of concentrations was utilized to react with LB and SB at room temperature (RT, 30 °C). As shown in **Fig. 1a**, LB is comparatively stable in deionized water with only 152 mL  $\text{g}^{-1}$  of  $\text{H}_2$  liberated in 30 min at RT. At the same time, it exhibits faster hydrogen kinetics in the presence of  $\text{CoCl}_2$ , steadily releasing more than 4000 mL  $\text{g}^{-1}$  of  $\text{H}_2$  under the same conditions. For example, it takes merely ~27 minutes for LB to complete the hydrolysis reaction, and there is nearly 4170 mL  $\text{g}^{-1}$  of  $\text{H}_2$  released ultimately. The corresponding  $\text{H}_2$  generation rate is increased to 155 mL  $\text{min}^{-1}$   $\text{g}^{-1}$ , which is higher than that (2 mL  $\text{min}^{-1}$   $\text{g}^{-1}$ ) of  $\text{CoCl}_2$ -free LB, as illustrated in **Fig. 1b**. As the concentration of  $\text{CoCl}_2$

increases to 0.1 wt%, the H<sub>2</sub> generation rate indicates a visible promotion increasing from 155 to 449 mL min<sup>-1</sup> g<sup>-1</sup>, and the reaction time is reduced to 9 minutes. The full hydrogen release would be realized within 6 min at the concentration of CoCl<sub>2</sub> more than 0.15 wt%. With the addition of 0.5 wt% CoCl<sub>2</sub> solution, the hydrolysis of LB could achieve a hydrogen yield of ~4000 mL g<sup>-1</sup> H<sub>2</sub> in only 1 min. The influence of CoCl<sub>2</sub> concentration is clearly presented by both the increasing slope values of hydrogen generation plots and the decreasing reaction completing time reduced from 26 to 1 min at the concentration of CoCl<sub>2</sub> solution increasing from 0.05 to 0.5 wt%. **Fig. 1b** presents the hydrogen generation rate of LB in the presence of CoCl<sub>2</sub> at the concentration ranging from 0.05 to 0.50 wt%, which is positively correlated to the concentration of CoCl<sub>2</sub>. Exactly, a well-controlled hydrogen generation rate ranging from 155, 449, 713, 884, 902 to 3725 mL min<sup>-1</sup> g<sup>-1</sup> H<sub>2</sub> is realized by tailoring the concentration of CoCl<sub>2</sub> from 0.05, 0.10, 0.15, 0.20, 0.25, to 0.50 wt%, thus matching the demands for fuel cells of various power.

Resembling LiBH<sub>4</sub>, the hydrolysis of SB also shows controllable hydrogen kinetics in the presence of CoCl<sub>2</sub>. Though the hydrogen yield of SB is lower than that of LB, it exhibits a more precisely controlled hydrogen generation rate with more negligible heat effect during the hydrolysis process ( $\text{NaBH}_4 + 4\text{H}_2\text{O} \rightarrow \text{NaBO}_2 \cdot 2\text{H}_2\text{O} + 4\text{H}_2 + 217 \text{ kJ mol}^{-1}$ ,  $\text{LiBH}_4 + 4\text{H}_2\text{O} \rightarrow \text{LiBO}_2 \cdot 2\text{H}_2\text{O} + 4\text{H}_2 + 289.9 \text{ kJ mol}^{-1}$ ). More specifically, the hydrogen behaviors of SB were investigated with different concentrations of CoCl<sub>2</sub> solution. According to **Fig. 1c**, the final value of hydrogen yield of SB hydrolysis is ~2580 mL g<sup>-1</sup> H<sub>2</sub> with a conversion rate of ~100% at a concentration of CoCl<sub>2</sub> varied

from 0.05 to 0.25 wt%. Such conversion rate illustrates the feasibility of SB as the hydrogen source of portable mobile powers. Correspondingly, the reaction completing time is reduced from ca. 28 min to ca. 1 min. However, an exception occurs when the CoCl<sub>2</sub> solution is 0.5 wt%. The catalytic reaction is completed within merely ~0.5 minutes, delivering a hydrogen yield of about 2350 mL g<sup>-1</sup> H<sub>2</sub>, which is slightly less than the theoretical value of 2590 mL g<sup>-1</sup> H<sub>2</sub>. This may be attributed to the formation of a large number of byproducts (NaBO<sub>2</sub>·xH<sub>2</sub>O), thus rapidly depositing on the surface of SB to prevent the complete contact of the borohydride with the reaction solution. **Fig. 1d** presents the hydrogen generation rate of SB in CoCl<sub>2</sub> solution with a concentration ranging from 0.05 to 0.50 wt%. Resembling LB hydrolysis, the hydrogen kinetics of SB is also positively correlated with the concentration of CoCl<sub>2</sub>. When the catalyst concentration is 0.05 wt%, the rate of hydrogen generation is 93 mL min<sup>-1</sup> g<sup>-1</sup>. Afterward, the hydrogen rate is increased from 646 to 1841 mL min<sup>-1</sup> g<sup>-1</sup> when the concentration of CoCl<sub>2</sub> is increased from 0.10 to 0.25 wt%. However, there is a enormous shift when the concentration of catalyst is 0.50 wt%, wherein the hydrolysis of SB provides a high hydrogen-release rate of 4243 mL min<sup>-1</sup> g<sup>-1</sup>, even higher than that of LB (3725 mL min<sup>-1</sup> g<sup>-1</sup>) under the same conditions.

To assess the efficiency of CoCl<sub>2</sub>, the hydrogen behaviors of SB were further investigated at a temperature varied from 15 to 35 °C, as illustrated in **Fig. 1e**. For the practical application, the concentration of CoCl<sub>2</sub> solution was determined to be 0.1 wt%. According to the Arrhenius equation<sup>28-29</sup>, the apparent activation energy of SB with the catalysis of CoCl<sub>2</sub> was calculated to be 33.5 kJ mol<sup>-1</sup> (**Fig. 1f**), which is in the range of

30-90 kJ mol<sup>-1</sup> found for metal-catalyzed hydrolysis of SB and AB (ammonia borane)

22

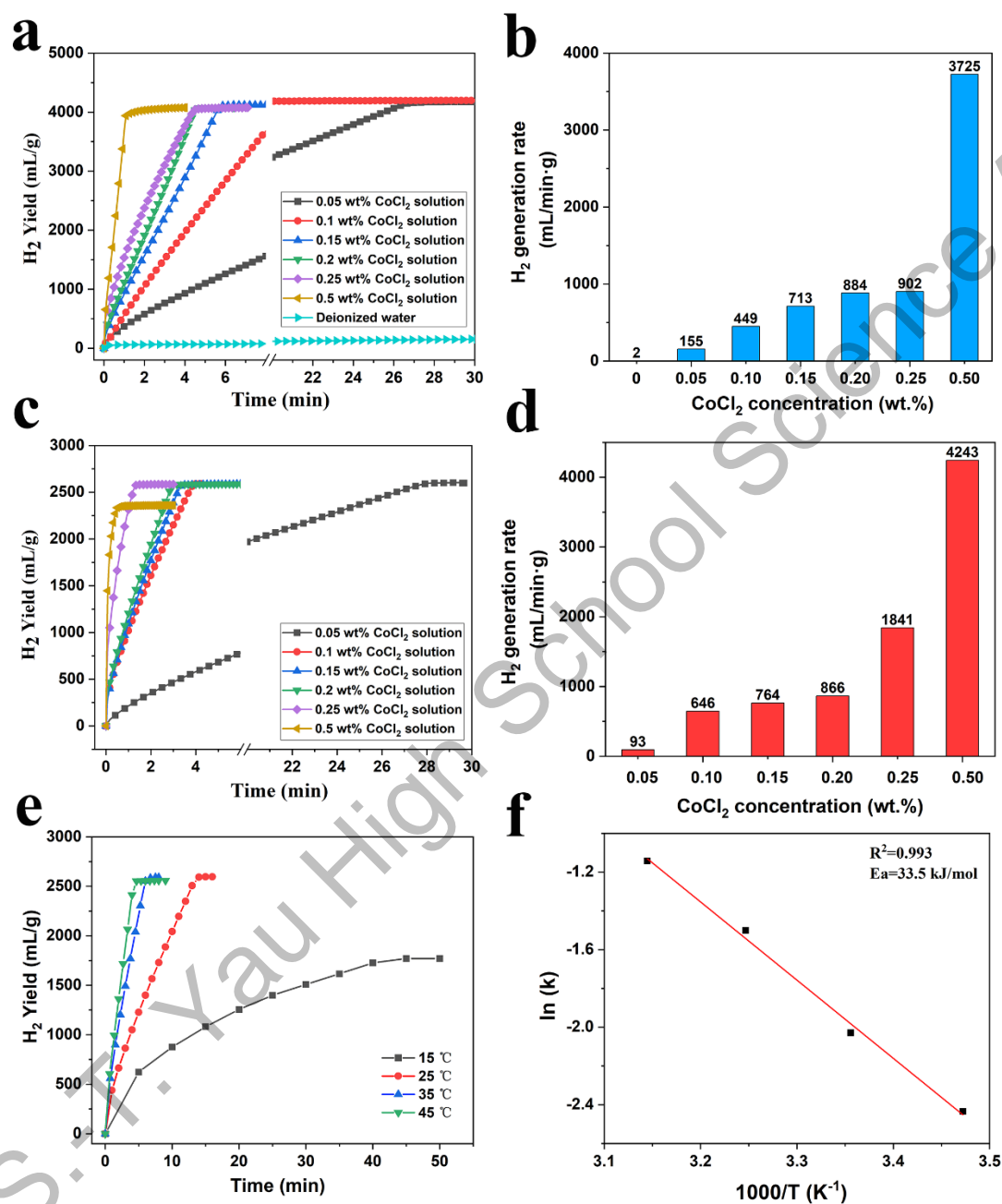


**Fig. 1** Hydrogen generation plots (a) and hydrogen generation rate (b) of LB in an excess amount of CoCl<sub>2</sub> solution with different concentrations. Hydrogen generation plots (c) and hydrogen generation rate (d) of SB in an excess amount of CoCl<sub>2</sub> solution with different concentrations. (e) Hydrogen production plots of SB versus time (min) with 0.1 wt% of CoCl<sub>2</sub> solution in the

temperature range of 15-45 °C. (f) Arrhenius plots of  $\ln k$  vs. the reciprocal absolute temperature  $1/T$  in the temperature range of 15-45 °C.

### **3.2 The gravimetric hydrogen density of NaBH<sub>4</sub>-based system with a stoichiometric amount of CoCl<sub>2</sub> solution**

To improve the endurance ability of portable fuel systems, especially for special applications such as outdoor small power generators, uncrewed airplanes, underwater vehicles, and so on, both good hydrogen yield and desirable GHD are of significance. In the present work, to determine the optimum GHD of LB or SB based fuel system, stoichiometric amount of CoCl<sub>2</sub> aqueous solution (according to Eqn. 1, H<sub>2</sub>O/(LB or SB) = 2-6 mol/mol) was dropped to react with LB or SB at RT. According to **Fig. 2a**, the hydrolysis rate of LiBH<sub>4</sub> is rapid at H<sub>2</sub>O/LB = 2-6 mol/mol, correlating to an initial hydrogen generation rate from 1474 to 2374 mL min<sup>-1</sup> g<sup>-1</sup> H<sub>2</sub>. According to **Fig. 2b**, with all components considered, the maximum GHD of the hydrolysis system is 8.7 wt.% H<sub>2</sub> at H<sub>2</sub>O/LiBH<sub>4</sub> = 2 mol/mol. However, its hydrogen yield is just ~63%. Such yield is attributed to the evaporation of water because the reaction is extremely exothermic, and the reaction system has a poor heat capacity<sup>30-31</sup>. Therefore, the molar ratio of H<sub>2</sub>O/LB was further increased from 3 to 6 mol/mol. The H<sub>2</sub> conversion yield of LB is positively proportionate to the amount of CoCl<sub>2</sub> solution, reaching the highest point of 89% at H<sub>2</sub>O/LB = 6 mol/mol. However, the GHD of the solid-liquid reaction system declines when the amount increases because the mass of H<sub>2</sub> generated is smaller than the mass of water and CoCl<sub>2</sub> used during the reaction. Therefore, the hydrolysis system possesses the optimal hydrogen behaviors at H<sub>2</sub>O/LiBH<sub>4</sub> = 4 mol/mol with the

GHD of ~7.2% and a massive hydrogen yield of 83%. Still, because of the acuteness of the hydrolysis reaction, it is hard to be manipulated at the beginning. Furthermore, after its initial rapidity the reaction turns slow. These lead to a poor yield of effective hydrogen. The unsatisfactory kinetics may be attributed to the formation of the adhesive  $\text{LiBO}_2$ -based byproduct on the surface of LB and therefore inhibits the full hydrolysis reaction<sup>32 33</sup>.

Differ from LB, the hydrolysis reaction of SB is more controllable in the presence of a stoichiometric amount of  $\text{CoCl}_2$  solution. As shown in **Fig. 2c**, when the molar ratio of  $\text{H}_2\text{O}:\text{SB}$  differentiates from 2 to 6 mol/mol, the  $\text{H}_2$  yield increases from  $1400 \text{ mL g}^{-1}$  in 60 min to  $2590 \text{ mL g}^{-1}$  (100% of fuel conversion) within 1.3 min. The effect of the molar ratio of  $\text{H}_2\text{O}/\text{SB}$  significantly influences the hydrogen yield and hydrogen release kinetics. For 1:3 of  $\text{SB}:\text{H}_2\text{O}$ , a hydrogen yield of  $2111 \text{ mL g}^{-1}$  could be obtained in 60 min, whereas the reaction completing time is shortened to below 2 min with a hydrogen generation rate of  $1507\text{-}2442 \text{ mL g}^{-1} \text{ min}^{-1}$  as the mole ratio of  $\text{H}_2\text{O}/\text{SB}$  increases from 4 to 6 mol/mol. According to **Fig. 2d**, the SB-based hydrolysis system holds the highest optimal GHD of 7.0 wt% as well as a considerable hydrogen yield of  $2525 \text{ mL g}^{-1}$  (97% of fuel conversion).

Compared with LB, SB that enables all hydrogen to release in a moderate reaction rate with a stoichiometry of  $\text{CoCl}_2$  solution, it may be more suitable for SB to apply in UAV or other outdoor portable electronic devices. With less water usage, the entire hydrogen density of the SB-based hydrogen system will be greatly enhanced. In this

regard, UAV powered by fuel cells will have stronger endurance with the same mass of fuel load.

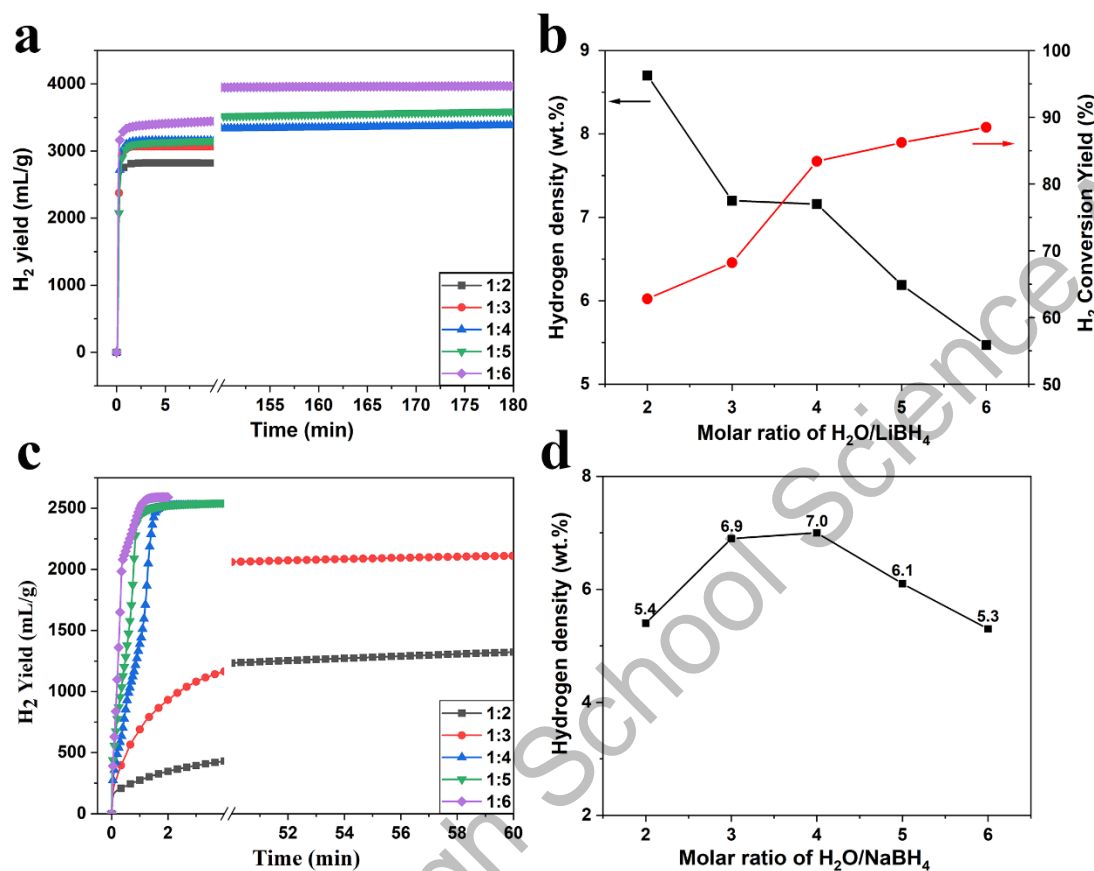


**Fig. 2** Hydrogen generation curves (a), and hydrogen conversion rate and GHD (b) of LB-based system at H<sub>2</sub>O/LB = 2-6 mol/mol in the presence of 2 wt% CoCl<sub>2</sub> solution. Hydrogen kinetic curves (c) and GHD (b) of SB-based system with a molar ratio of H<sub>2</sub>O/LB being 2-6 mol/mol in the presence of 5 wt% CoCl<sub>2</sub> solution.

### 3.3 The hydrogen generator integrated with a PEM fuel-cell stack and the application in LED

With sufficient investigations on the hydrogen generation kinetics of the borohydrides (LB and SB), it is possible for us to design an integrated fuel cell system

that enables the hydrogen generation rate to match the consumption of the PEM fuel-cell stack. As shown in **Fig. 3**, a fuel cell LED system integration consists of three parts: a hydrogen generator, a 30 W PEM fuel cell stack, and a 15 W LED display screen. For the hydrogen generation part, 0.1 wt% of  $\text{CoCl}_2$  solution is injected into the hydrogen generator to react with LB or SB to generate hydrogen. The hydrogen released is exhausted through a pipe and enters into the fuel cell stack. Inside the 30 W PEM fuel cell stack, a hydrogen flow rate  $\geq 0.4 \text{ L min}^{-1} \text{ H}_2$  ( $0.45 \text{ L min}^{-1}$  for LB and  $0.65 \text{ L min}^{-1}$  for SB) is needed to react with oxygen from the air with water as the only product, enabling the fuel cell to operate at rated power. Concerning the electronic appliance, the electricity is generated in real-time by the fuel cell, which is conveyed to a 15 W LED display screen and enables it to operate steadily.

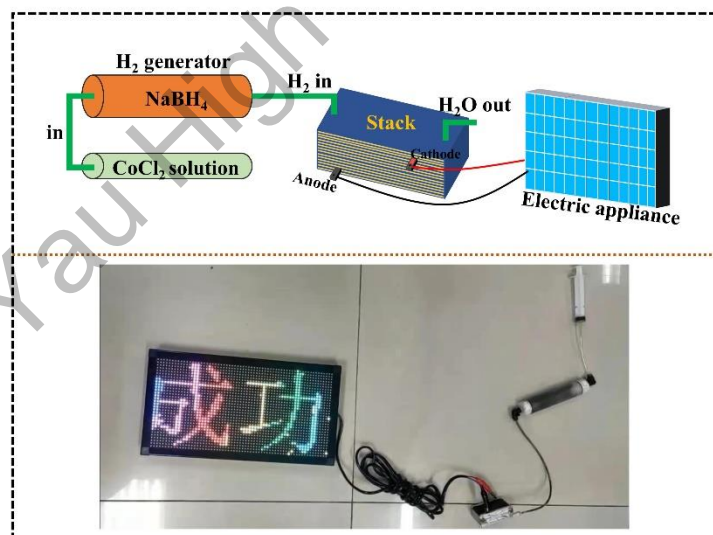


**Fig. 3** Schematic of the fuel cell system consisting of hydrogen generator, a fuel cell stack, and electric appliance. Inset: a fuel cell LED system integration operated with SB hydrogen source.

For the actual application of this integrated system, it's necessary to take the heat effect with massive fuel during the hydrolysis process into account. Thus, the temperature of the reaction systems was measured over the hydrolysis process. As shown in **Fig. 4a**, the reaction temperature plots vs. the time for 1g LB in 20 mL of 0.1 wt%  $\text{CoCl}_2$  solution are present. As the reaction continues, the temperature gradually increases from 24 °C to 80 °C after 4.2 min and then is followed by a decrease. The peak temperature is 80 °C, and the significant heat effect accelerates the reaction kinetics of LB, especially in the later stage. For SB hydrolysis, 2 g of SB is used to react with 20 mL of 0.1 wt%  $\text{CoCl}_2$  solution to produce an equivalent amount of hydrogen as LB. As shown in **Fig. 4b**, the hydrolysis of SB is more stable than LB, and the reaction temperature is no more than 40 °C over the entire hydrolytic process. For this moderate temperature range, it is able to supply a steady hydrogen flow for the fuel cell stack. Hence, the SB is a preferable material to act as the hydrogen fuel for PEM fuel cell integrated system. As expected, SB catalyzed by  $\text{CoCl}_2$  solution can stably supply hydrogen to PEM fuel cell stack, therefore powering a 15 W LED display screen (**Fig. 3**).

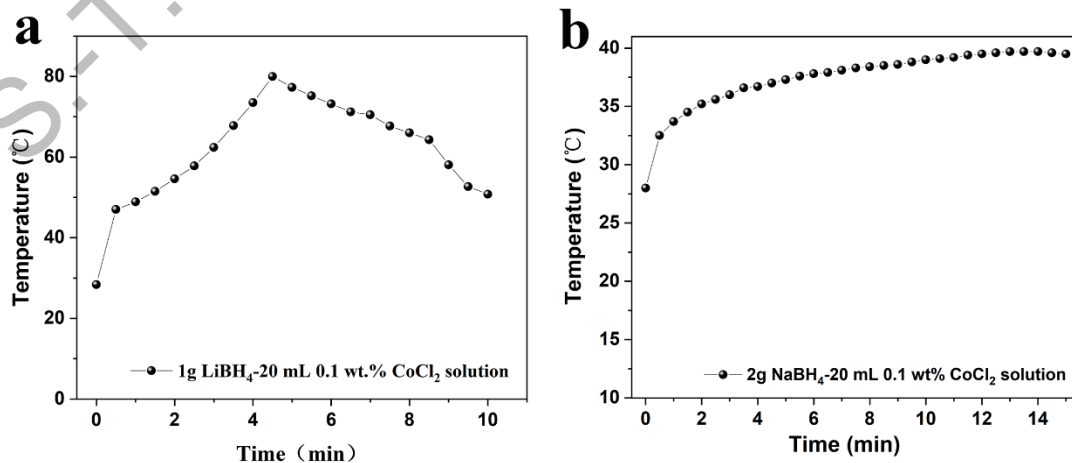


**Fig. 4** (a) Temperature change as a function of reaction time as 1g of LB reacts with 20 mL 0.1 wt% CoCl<sub>2</sub> solution. (b) Temperature change as a function of reaction time as 2g of SB reacts with 20 mL 0.1 wt% CoCl<sub>2</sub> solution.

### 3.4 Characterization of spent fuels and regeneration

One of the most advantages that the electricity generated through hydrolysis of borohydrides may be from renewable energy. The hydrolysis of borohydrides spontaneous process with pure hydrogen released, which could be well controlled to satisfy the requirements of different power PEM fuel cells by catalysis. For SB hydrolysis with CoCl<sub>2</sub> catalyst, the by-product after drying was characterized by XRD and FTIR. As expected, there are no peaks attributed to SB, and the diffraction peaks observed in **Fig. 5a** are mainly indexed to NaBO<sub>2</sub>·2H<sub>2</sub>O, matching well with those in the PDF card (NaBO<sub>2</sub>·2H<sub>2</sub>O: 00-006-0122). Notably, the other peaks denoted by “plus” are assigned to Na<sub>2</sub>CIB(OH)<sub>4</sub>, formed presumably from the introduction of CoCl<sub>2</sub>. Moreover, analysis of the FT-IR spectra (**Fig. 5b**) from the by-products of the samples of SB:H<sub>2</sub>O = 1:4 with 5 wt% of CoCl<sub>2</sub> solution and 2g SB-20mL of 0.1 wt% CoCl<sub>2</sub> solution demonstrates the stretching vibrations of B-O at 1290 and 900-700 cm<sup>-1</sup>, and bending vibration of B-O-H at 1190 cm<sup>-1</sup>, which are determined to be NaBO<sub>2</sub>·2H<sub>2</sub>O as the data reported previously<sup>12, 34</sup>.

In recent years, Ouyang et al.<sup>23, 34-40</sup> have been working on the regeneration of borohydrides and made significant progress in recycling NaBO<sub>2</sub>·xH<sub>2</sub>O and other spent fuels. Here, we conceive a closed materials loop for hydrogen generation, storage, and utilization with the couple of SB/LB hydrolysis and regeneration, as shown in **Fig. 5c**.

For the regeneration of the borohydride-based spent fuels, it may use solar energy and other renewable energy to convert  $H^+$  in coordinated water bound to  $MBO_2$  towards precious  $H^-$  in  $MBH_4$  by ball milling method. In this regard, the application cost of SB or LB may be greatly reduced while acting hydrogen source for PEMFCs.

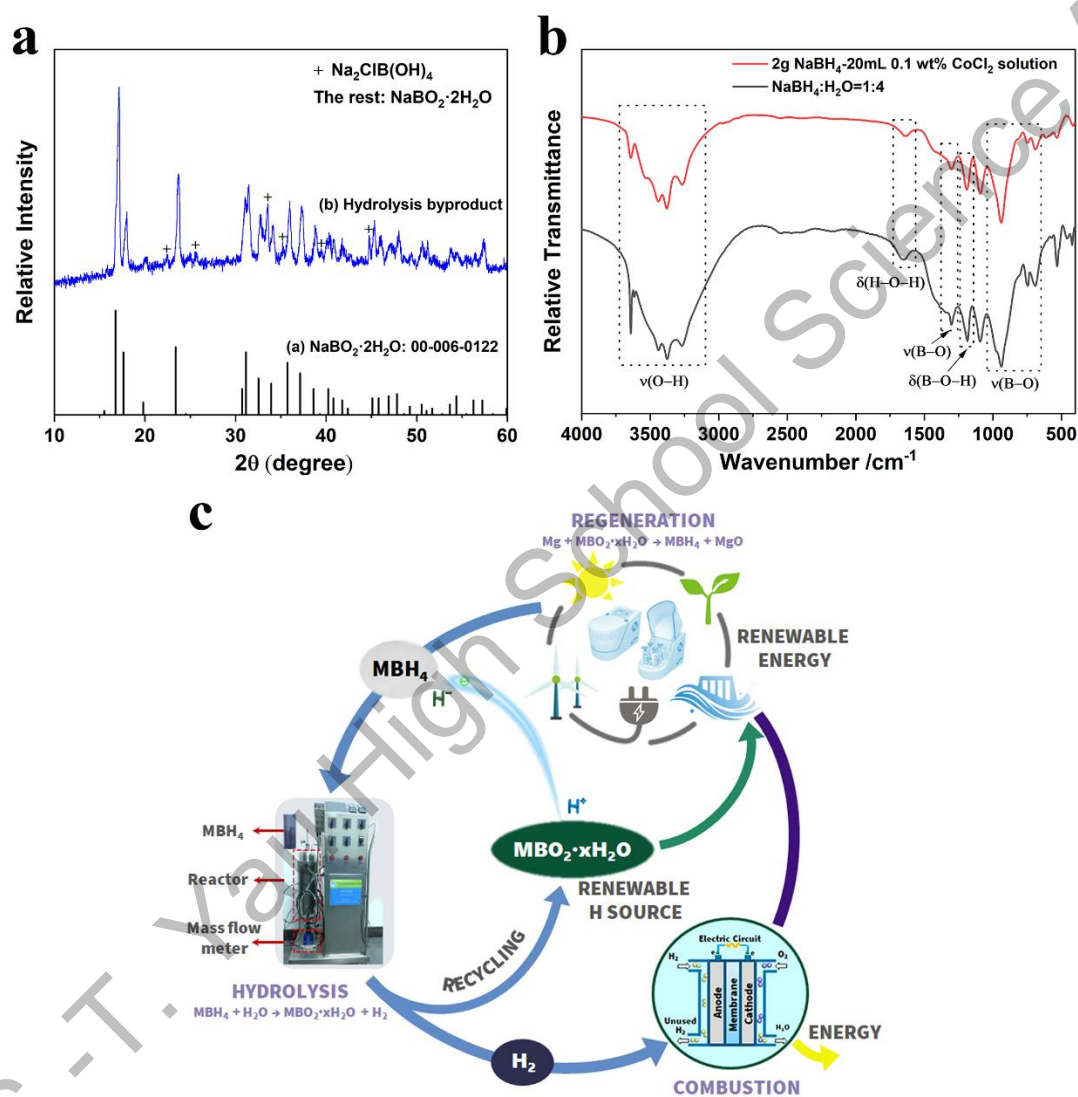


**Fig. 5** (a) XRD patterns of hydrolysis product using 5 wt% of  $CoCl_2$  solution with a molar ratio of  $H_2O/SB$  being 4 mol/mol. (b) FTIR spectra obtained from hydrolysis products using 2g SB reacting with 20 mL 0.1 wt%  $CoCl_2$  solution and using 5 wt% of  $CoCl_2$  solution in a molar ratio

of  $\text{H}_2\text{O}/\text{SB} = 4$  mol/mol. (c) A closed materials loop for hydrogen cycle with the couple of SB/LB hydrolysis and regeneration.

#### 4 Conclusions

In summary, the hydrolysis behaviors of LB and SB in the presence of  $\text{CoCl}_2$  solution were investigated in the present work. A precisely controlled hydrogen generation rate up to  $4.2 \text{ L min}^{-1}$  was achieved by tailoring the concentration of  $\text{CoCl}_2$  solution, which may meet the requirements of different power PEMFCs. Based on the hydrogen kinetic studies, a PEM fuel cell integrated with SB hydrogen source was developed. Notably, a steady hydrogen flow (over  $0.4 \text{ L min}^{-1} \text{ H}_2$ ) can be achieved to power a 30 W PEMFC that enables a 15 W LED display screen to light up steadily by reacting SB with 0.1 wt%  $\text{CoCl}_2$  solution. By reacting LB/SB with a stoichiometric amount of  $\text{CoCl}_2$  solution, a desirable GHD of 7.0 wt%  $\text{H}_2$  with  $\sim 100\%$  fuel conversion was realized at  $\text{H}_2\text{O}:\text{SB} = 4:1$ . The by-product after hydrolysis reaction was determined to be  $\text{MBO}_2 \cdot x\text{H}_2\text{O}$ . By using green energy, it is convenient to convert renewable hydrogen from coordinated water bound to  $\text{MBO}_2$  to expensive  $\text{H}^-$  stored in  $\text{MBH}_4$  by ball milling  $\text{MBO}_2 \cdot x\text{H}_2\text{O}$  with Mg-based reducing agents, thereby greatly lowering the application cost. The study on LED display screen powered by SB-based hydrogen source integrated with 30 W fuel cell and the optimization of the hydrolysis reaction will lay a solid foundation for the practical application of UAV driven by hydrogen energy with ideal flight endurance.

## Acknowledgements

This work was financially supported by the Foundation for Innovative Research Groups of the National Natural Science Foundation of China (No. NSFC51621001).

## References

1. Zinkle, S. J.; Was, G. S., Materials challenges in nuclear energy. *Acta Materialia* **2013**, *61* (3), 735-758.
2. Romero, E.; Novoderezhkin, V. I.; van Grondelle, R., Quantum design of photosynthesis for bio-inspired solar-energy conversion. *Nature* **2017**, *543* (7645), 355-365.
3. Kabir, E.; Kumar, P.; Kumar, S.; Adelodun, A. A.; Kim, K.-H., Solar energy: Potential and future prospects. *Renewable and Sustainable Energy Reviews* **2018**, *82*, 894-900.
4. Schlapbach, L.; Zuttel, A., Hydrogen-storage materials for mobile applications. *Nature* **2001**, *414* (6861), 353-358.
5. Zuttel, A.; Callini, E.; Kato, S.; Atakli, Z. O. K., Storing Renewable Energy in the Hydrogen Cycle. *Chimia (Aarau)* **2015**, *69* (12), 741-745.
6. Stamenkovic, V. R.; Mun, B. S.; Arenz, M.; Mayrhofer, K. J. J.; Lucas, C. A.; Wang, G.; Ross, P. N.; Markovic, N. M., Trends in electrocatalysis on extended and nanoscale Pt-bimetallic alloy surfaces. *Nature Materials* **2007**, *6* (3), 241-247.
7. Michael Hirscher, a. T. A., \*[b] and Shin-ichi Orimo\*[c], Hydrogen energy. *Chemphyschem* **2019**, *20* (2), 1157.
8. Flipsen, S. F. J.; Spitas, C., Direct methanol fuel cells: A database-driven design procedure. *Journal of Power Sources* **2011**, *196* (20), 8472-8483.
9. Xia, Z. T.; Chan, S. H., Feasibility study of hydrogen generation from sodium borohydride solution for micro fuel cell applications. *Journal of Power Sources* **2005**, *152*, 46-49.
10. Yeom, J.; Jayashree, R. S.; Rastogi, C.; Shannon, M. A.; Kenis, P. J. A., Passive direct formic acid microfabricated fuel cells. *Journal of Power Sources* **2006**, *160* (2), 1058-1064.
11. Ouyang, L. Z.; Chen, K.; Jiang, J.; Yang, X. S.; Zhu, M., Hydrogen storage in light-metal based systems: A review. *Journal of Alloys and Compounds* **2020**, *829*, 38.
12. Chen, W.; Ouyang, L. Z.; Liu, J. W.; Yao, X. D.; Wang, H.; Liu, Z. W.; Zhu, M., Hydrolysis

and regeneration of sodium borohydride (NaBH<sub>4</sub>) - A combination of hydrogen production and storage. *Journal of Power Sources* **2017**, 359, 400-407.

13. Bernhard, K. J. M. T., Solid-state hydrogen storage. **2009**, 12 (5), 51.
14. Orimo, S. I.; Nakamori, Y.; Eliseo, J. R.; Zuttel, A.; Jensen, C. M., Complex hydrides for hydrogen storage. *Chemical Review* **2007**, 107 (10), 4111-4132.
15. Lang, C.; Jia, Y.; Yao, X., Recent advances in liquid-phase chemical hydrogen storage. *Energy Storage Materials* **2020**, 26, 290-312.
16. Wang, C.; Astruc, D., Recent developments of nanocatalyzed liquid-phase hydrogen generation. *Chemical Society Review* **2021**, 50, 3437-3484.
17. Zuttel, A.; Wenger, P.; Rentsch, S.; Sudan, P.; Maun, P.; Emmenegger, C., LiBH<sub>4</sub> a new hydrogen storage material. *Journal of Power Sources* **2003**, 118 (1-2), 1-7.
18. Zuttel, A.; Borgschulte, A.; Orimo, S.-I., Tetrahydroborates as new hydrogen storage materials. *Scripta Materialia* **2007**, 56 (10), 823-828.
19. Maun, P.; Buchter, F.; Friedrichs, O.; Remhof, A.; Biemann, M.; Zwicky, C. N.; Zuttel, A., Stability and reversibility of LiBH<sub>4</sub>. *Journal of Physical Chemistry B* **2008**, 112 (3), 906-910.
20. Ouyang, L. Z.; Jiang, J.; Chen, K.; Zhu, M.; Liu, Z. W., Hydrogen Production via Hydrolysis and Alcoholysis of Light Metal-Based Materials: A Review. *Nano-Micro Letters* **2021**, 13 (1).
21. Deng, J.; Sun, B.; Xu, J.; Shi, Y.; Xie, L.; Zheng, J.; Li, X., A monolithic sponge catalyst for hydrogen generation from sodium borohydride solution for portable fuel cells. *Inorganic Chemistry Frontiers* **2021**, 8 (1), 35-40.
22. Li, L.; Li, S.; Tan, Y.; Tang, Z.; Cai, W.; Guo, Y.; Li, Q.; Yu, X., Hydrogen Generation from Hydrolysis and Methanolysis of Guanidinium Borohydride. *The Journal of Physical Chemistry C* **2012**, 116 (27), 14218-14223.
23. Ouyang, L. Z.; Chen, W.; Liu, J. W.; Felderhoff, M.; Wang, H.; Zhu, M., Enhancing the Regeneration Process of Consumed NaBH<sub>4</sub> for Hydrogen Storage. *Advanced Energy Materials* **2017**, 7 (19).
24. Zhang, X.; Zhang, Q.; Xu, B.; Liu, X.; Zhang, K.; Fan, G.; Jiang, W., Efficient Hydrogen Generation from the NaBH<sub>4</sub> Hydrolysis by Cobalt-Based Catalysts: Positive Roles of Sulfur-Containing Salts. *ACS Applied Materials & Interfaces* **2020**, 12 (8), 9376-9386.
25. Demirci, U. B.; Akdim, O.; Hannauer, J.; Chamoun, R.; Miele, P., Cobalt, a reactive metal in

releasing hydrogen from sodium borohydride by hydrolysis: A short review and a research perspective. *Science China Chemistry* **2010**, *53* (9), 1870-1879.

26. Chen, B.; Chen, S.; Bandal, H. A.; Appiah-Ntiamoah, R.; Jadhav, A. R.; Kim, H., Cobalt nanoparticles supported on magnetic core-shell structured carbon as a highly efficient catalyst for hydrogen generation from NaBH<sub>4</sub> hydrolysis. *International Journal of Hydrogen Energy* **2018**, *43* (19), 9296-9306.

27. Chen, K.; Ouyang, L. Z.; Wang, H.; Liu, J. W.; Shao, H. Y.; Zhu, M., A high-performance hydrogen generation system: Hydrolysis of LiBH<sub>4</sub>-based materials catalyzed by transition metal chlorides. *Renewable Energy* **2020**, *156*, 655-664.

28. Huang, M.; Ouyang, L.; Ye, J.; Liu, J.; Yao, X.; Wang, H.; Shao, H.; Zhu, M., Hydrogen generation via hydrolysis of magnesium with seawater using Mo, MoO<sub>2</sub>, MoO<sub>3</sub> and MoS<sub>2</sub> as catalysts. *Journal of Materials Chemistry A* **2017**, *5* (18), 8566-8575.

29. Wang, M.; Ouyang, L.; Peng, C.; Zhu, X.; Zhu, W.; Shao, H.; Zhu, M., Synthesis and hydrolysis of NaZn(BH<sub>4</sub>)<sub>3</sub> and its ammoniates. *Journal of Materials Chemistry A* **2017**, *5* (32), 17012-17020.

30. Kojima, Y.; Kawai, Y.; Kimbara, M.; Nakanishi, H.; Matsumoto, S., Hydrogen generation by hydrolysis reaction of lithium borohydride. *International Journal of Hydrogen Energy* **2004**, *29* (12), 1213-1217.

31. Kong, V. C. Y.; Foulkes, F. R.; Kirk, D. W.; Hinatsu, J. T., Development of hydrogen storage for fuel cell generators. i: Hydrogen generation using hydrolysis hydrides. *International Journal of Hydrogen Energy* **1999**, *24* (7), 665-675.

32. Li, C.; Peng, P.; Zhou, D. W.; Wan, L., Research progress in LiBH<sub>4</sub> for hydrogen storage: A review. *International Journal of Hydrogen Energy* **2011**, *36* (22), 14512-14526.

33. Zhu, L.; Kim, D.; Kim, H.; Masel, R. I.; Shannon, M. A., Hydrogen generation from hydrides in millimeter scale reactors for micro proton exchange membrane fuel cell applications. *Journal of Power Sources* **2008**, *185* (2), 1334-1339.

34. Zhong, H.; Ouyang, L. Z.; Ye, J. S.; Liu, J. W.; Wang, H.; Yao, X. D.; Zhu, M., An one-step approach towards hydrogen production and storage through regeneration of NaBH<sub>4</sub>. *Energy Storage Materials* **2017**, *7*, 222-228.

35. Huang, M. J.; Zhong, H.; Ouyang, L. Z.; Peng, C. H.; Zhu, X. K.; Zhu, W. H.; Fang, F.; Zhu, M., Efficient regeneration of sodium borohydride via ball milling dihydrate sodium metaborate with

magnesium and magnesium silicide. *Journal of Alloys and Compounds* **2017**, 729, 1079-1085.

36. Zhu, Y. Y.; Ouyang, L. Z.; Zhong, H.; Liu, J. W.; Wang, H.; Shao, H. Y.; Huang, Z. G.; Zhu, M., Closing the Loop for Hydrogen Storage: Facile Regeneration of NaBH<sub>4</sub> from its Hydrolytic Product. *ANGEWANDTE CHEMIE-INTERNATIONAL EDITION* **2020**, 59 (22), 8623-8629.

37. Zhu, Y.; Ouyang, L.; Zhong, H.; Liu, J.; Wang, H.; Shao, H.; Huang, Z.; Zhu, M., Efficient Synthesis of Sodium Borohydride: Balancing Reducing Agents with Intrinsic Hydrogen Source in Hydrated Borax. *ACS Sustainable Chemistry & Engineering* **2020**, 8 (35), 13449-13458.

38. Zhong, H.; Ouyang, L. Z.; Zeng, M. Q.; Liu, J. W.; Wang, H.; Shao, H. Y.; Felderhoff, M.; Zhu, M., Realizing facile regeneration of spent NaBH<sub>4</sub> with Mg-Al alloy. *Journal of Materials Chemistry A* **2019**, 7 (17), 10723-10728.

39. Lang, C. G.; Jia, Y.; Liu, J. W.; Wang, H.; Ouyang, L. Z.; Zhu, M.; Yao, X. D., NaBH<sub>4</sub> regeneration from NaBO<sub>2</sub> by high-energy ball milling and its plausible mechanism. *International Journal of Hydrogen Energy* **2017**, 42 (18), 13127-13135.

40. Chen, K.; Ouyang, L.; Zhong, H.; Liu, J.; Wang, H.; Shao, H.; Zhang, Y.; Zhu, M., Converting H<sup>+</sup> from coordinated water into H<sup>-</sup> enables super facile synthesis of LiBH<sub>4</sub>. *Green Chemistry* **2019**, 21 (16), 4380-4387.

2021 S.-T. Yau High School Science Award

致谢:

1. 选题来源于欧阳先生的研究主题：通过氢能使燃料电池产生电力作为载具的动力。
2. 论文主体由张浚祈撰写
3. 老师在学生完成论文写作后协助修改论文，无偿。
4. 其中因部分实验具有危险性（ $\text{LiBH}_4$  活性极高），由老师协助完成探索制氢动力学的实验。

2021 S.-T. Yau High School Science Award